



Air pollution exacerbates mild obstructive sleep apnea by disrupting nocturnal changes in lower-limb body composition: a cross-sectional study conducted in urban northern Taiwan

Yansu He ^a, Wen-Te Liu ^{b,c,d}, Shang-Yang Lin ^b, Zhiyuan Li ^e, Hong Qiu ^a, Steve Hung-Lam Yim ^f, Hsiao-Chi Chuang ^{c,d,g}, Kin Fai Ho ^{a,e,*}

^a JC School of Public Health and Primary Care, The Chinese University of Hong Kong, Hong Kong, China

^b Research Center of Sleep Medicine, College of Medicine, Taipei Medical University, Taipei, Taiwan

^c School of Respiratory Therapy, College of Medicine, Taipei Medical University, Taipei, Taiwan

^d Division of Pulmonary Medicine, Department of Internal Medicine, Shuang Ho Hospital, Taipei Medical University, Taipei, Taiwan

^e Institute of Environment, Energy and Sustainability, The Chinese University of Hong Kong, Hong Kong, China

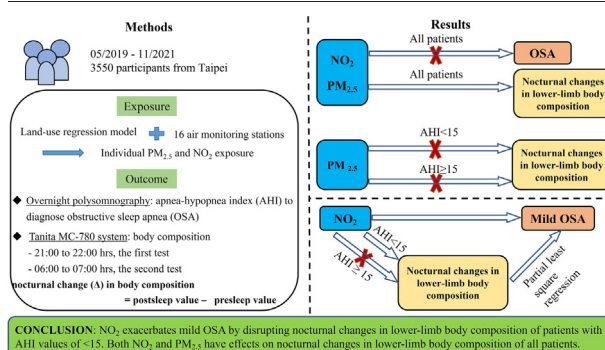
^f The Asian School of the Environment, Nanyang Technological University, Singapore

^g Cell Physiology and Molecular Image Research Center, Wan Fang Hospital, Taipei Medical University, Taipei, Taiwan

HIGHLIGHTS

- NO₂ and PM_{2.5} had short- and long-term effects on lower-limb body composition.
- NO₂ but not PM_{2.5} had short- and long-term effects on mild-OSA.
- PLSR addresses the collinearity between lower-limb body compositions.
- Combined effects of nocturnal changes in body composition on OSA were evaluated.
- NO₂ affected mild OSA by disrupting nocturnal changes in body composition.

GRAPHICAL ABSTRACT



ARTICLE INFO

Editor: Pavlos Kassomenos

Keywords:

Spatiotemporal model
Nocturnal changes in body composition
Partial least squares regression
Polysomnography
Bioelectric impedance analysis

ABSTRACT

Background: Few studies have explored the role of body composition linking air pollution to obstructive sleep apnea (OSA).

Objective: To estimate the effects of air pollution on body composition and OSA, and that of body composition on OSA.

Methods: This study included 3550 individuals. A spatiotemporal model estimated personal exposure. Nocturnal changes in body composition were assessed through bioelectric impedance analysis. OSA was diagnosed using polysomnography. A generalized linear model was used to evaluate the absolute nocturnal changes in body composition associated with an interquartile range (IQR) increase in pollutants. A generalized logistic model was used to estimate odds ratios (ORs) of mild-OSA compared to non-OSA. Association between body composition and apnea-hypopnea index (AHI) was investigated through partial least squares (PLS) regression.

Results: Nocturnal changes in lower-limb body composition were associated with NO₂ and PM_{2.5} in all patients. In participants with AHI <15, both short- and long-term NO₂ exposures affected body composition and mild-OSA, while PM_{2.5} was not associated with either outcome. In a PLS model incorporating eight NO₂-associated lower-limb

Abbreviations: AHI, apnea-hypopnea index;; OSA, obstructive sleep apnea; PM_{2.5}, particulate matter with an aerodynamic diameter of ≤2.5 μm; NO₂, nitrogen dioxide; IQR, interquartile range; PLS, partial least squares..

* Corresponding author at: The Jockey Club School of Public Health and Primary Care, The Chinese University of Hong Kong, Hong Kong, China.

E-mail address: kfho@cuhk.edu.hk (K.F. Ho).

<https://dx.doi.org/10.1016/j.scitotenv.2023.163969>

Received 9 January 2023; Received in revised form 23 April 2023; Accepted 2 May 2023

Available online 9 May 2023

0048-9697/© 2023 Elsevier B.V. All rights reserved.

parameters, the variable importance projection scores (VIP) of left leg impedance (LLIMP), predicted muscle mass (LLPMM), fat-free mass (LLFFM), and right leg impedance (RLIMP) exceeded 1; the corresponding coefficients ranked in the top four for AHI prediction. The adjusted OR (mild vs. non-OSA) was 1.67 (95 % CI: 1.36–2.03) associated with an IQR increase in prediction value estimated from body compositions. Notably, the two-pollutant model investigating the effects of pollutants on body compositions revealed associations of four parameters (LLIMP, LLPMM, LLFFM, and RLIMP) with NO₂ in all lags, which indicates their indispensability in the association between NO₂ and AHI.

Conclusions: NO₂ exacerbates mild-OSA by disrupting nocturnal changes in lower-limb body composition of patients with AHI <15. PM_{2.5} was associated with nocturnal changes in lower-limb body composition but not with mild-OSA.

1. Introduction

The prevalence of obstructive sleep apnea (OSA), a common sleep disorder, is higher in men than in women (Reutrakul and Mokhlesi, 2017). Clinically, OSA is diagnosed using overnight polysomnography, which records intermittent collapse (apnea), partial blockage (hypopnea), intermittent hypoxia, and sleep fragmentation (Park et al., 2011). Internal risk factors for OSA include advanced age, sex, smoking, alcohol consumption, and craniofacial abnormalities (Punjabi, 2008). Differences in environmental factors such as air pollution may explain the variations in OSA prevalence across regions (Urbanik et al., 2020). A study conducted in Taiwan reported that 1-year NO₂ exposure increased the apnea–hypopnea index (AHI) value in all patients with OSA (Shen et al., 2018); by contrast, a study conducted in the United States reported an NO₂ exposure–induced AHI increase only in patients with moderate to severe OSA (Billings et al., 2019). In addition to the aforementioned study (Billings et al., 2019), two studies conducted in Taiwan have focused on the effects of PM_{2.5} on OSA (Cheng et al., 2019; He et al., 2022); these two studies included individuals regardless of their OSA status and revealed no association between PM_{2.5} and AHI. Yet, another study reported a strong association between PM_{2.5} and AHI increase in all patients with OSA (Shen et al., 2018). Thus, the effects of air pollution appear to vary across patients with different OSA severities.

Changes in nocturnal body composition, such as the movement of body fluids because of sleeping in the supine position, may predispose individuals to OSA. During sleep, certain volumes of body fluids flow from the legs to the neck, thus increasing the likelihood of pharyngeal obstruction (Redolfi et al., 2009). In a study conducted in patients with OSA, a nocturnal reduction in leg fluid volume was inversely correlated with an AHI increase ($r = -0.773$; $p < .001$) and nocturnal changes in neck circumference ($r = -0.588$, $p = .003$) (Redolfi et al., 2009). An inverse correlation between leg (left) fluid reduction and AHI was also corroborated in a study of patients with OSA and hypertension ($r = -0.734$; $p = .001$) (Kasai et al., 2014) and another study of patients with OSA and heart failure ($r = -0.881$; $p < .001$) (Yumino et al., 2010). As bidirectionally, chronic OSA exerts adverse effects on various organ systems, leading to multiple comorbidities, among which hypertension and diabetes have garnered considerable attention (Jordan et al., 2014). OSA and cardiovascular diseases markedly affect the mass of skeletal muscles throughout the body, thus increasing the likelihood of sarcopenia. Obesity and aging, with which OSA is associated, may aggravate the adverse effects of various chronic diseases on muscle mass (Volpato et al., 2014). A study conducted in Japan indicated that AHI was positively and negatively correlated with skeletal muscle mass index and density, respectively (Matsumoto et al., 2018). Another study suggested that AHI is negatively correlated with muscle mass percentage (Kosacka et al., 2013). However, in a study conducted in Australia, no correlation was found between AHI and muscle mass; nonetheless, fat mass was consistently associated with worsening AHI (Stevens et al., 2020).

The pathogenesis of muscle mass loss is complicated. In addition to aging and OSA, traffic fumes may have an adverse effect. The tiny irritating particles in traffic fumes can trigger inflammatory cytokines, which interfere with hormones and disrupt energy flow and muscle synthesis (Chuang et al., 2007). A Taiwanese study revealed that PM_{2.5} led to a reduction in the fat-free mass of the trunk and upper limbs but not lower limbs; however, it increased the fat mass of the aforementioned three parts of

the body (Chen et al., 2019). Another Taiwanese study that included multiple descriptive body composition parameters revealed that PM_{2.5} increased the fat percentage and fat mass of the right arm, whereas NO₂ decreased muscle mass and fat-free mass of the whole body and increased the fat percentage of lower limbs (Tung et al., 2021).

In light of the aforementioned findings, the current status of research on the association between air pollution and OSA showed inconsistent results. Taiwan is an ideal setting for the present study, since the average annual mean concentrations of NO₂ and PM_{2.5} in Taiwan have surpassed the WHO guidelines ever and again (Su et al., 2019). Additionally, body composition may be associated with long-term OSA. However, few studies have simultaneously explored the associations of air pollution with body composition and OSA and that of OSA with air pollution–induced changes in body composition. Therefore, in this study, we investigated the association between traffic-related air pollution and nocturnal changes in body composition and OSA; and that between these changes and OSA.

2. Methods

2.1. Ethical considerations

The study protocol was approved by the Joint Institutional Review Board of Taipei Medical University, Taiwan (approval number: N201910048). The study participants received no direct benefit for participation. The requirement for informed consent was waived by the Chinese University of Hong Kong Survey and Behavioral Research Ethics Committee.

2.2. Study participants

This cross-sectional study included individuals who were referred to the Sleep Center of Taipei Medical University Hospital for a polysomnography diagnostic test between May 2019 and November 2021. Individuals with diabetes, cardiovascular disease, bronchiectasis, chronic obstructive pneumonia disease, venous insufficiency, heart failure, renal failure, and under dialysis treatment were excluded from this study. The participants were from the urban areas of northern Taiwan.

2.3. Polysomnography

Overnight polysomnography (Embla N7000, Medcare, Iceland) was performed by certified sleep technicians at the Sleep Center of Taipei Medical University Hospital; the test duration was >6 h. Somnologica for Embletta™ (Medcare, Iceland) was used as an analytical software and the American Academy of Sleep Medicine (AASM) criteria were combined to score the apnea and hypopnea events experienced by the participants (Ruehland et al., 2009). The definitions of apnea and hypopnea events that are used to calculate the numbers of apnea and hypopnea events per hour (AHI, events/h) are various, therefore, the AASM criteria were used to define the events. An apnea event was defined as a decrease in the peak signal excursion by ≥ 90 % of the pre-event baseline for ≥ 10 s, whereas a hypopnea event was defined as a decrease in the peak signal excursion by ≥ 30 % of the pre-event baseline for ≥ 10 s. Peripheral mean oxygen saturation was measured through pulse oximetry (Wong

et al., 2021). Data regarding the participants' age, sex, body mass index (BMI), and neck and waist circumferences were collected from the hospital's medical records (Qiu et al., 2022).

2.4. Nocturnal changes in body composition

A Tanita MC-780 system (Tanita, Tokyo, Japan) was used to measure body composition through bioelectrical impedance (Ward, 2019) of the patients at the Sleep Center of Taipei Medical University Hospital. This system measures the contents of fat, muscle, and water in the body. The following indices were used for further analysis: body fat mass (fat weight), body fat percentage (body fat as a percentage of the total body weight), muscle mass (muscle weight), visceral fat (fat around the abdominal cavity and organs), bone mass (bone weight), fat-free mass (weight of all body components except fat), total body water (total amount of body fluids), basal metabolic rate (minimum energy required to function effectively at rest), physique rating (body fat/muscle mass ratio), metabolic age (a participant's basal metabolic rate [BMR] compared to the average of the BMRs of the participant's chronological age group), phase angle (alterations in cell membrane functions), and impedance (speed of electrical signals traveling through the human body [ohm]; note that lean tissue contains more water and electrolytes than fat tissue, so fitness is associated with higher electrical impedance) (Lemos and Gallagher, 2017). Nocturnal changes in the composition of four body parts were assessed: the whole body, the trunk, and the upper and lower limbs. All participants fasted for ≥ 3 h before fluid analysis. At the time (21:00 h to 22:00 h) of the first test, the participants were requested to empty their bladder and hold the test instrument's handle vertically down with both arms while keeping their inner thighs apart. Henceforward, eating and drinking were not allowed until the completion of the second-test, which was conducted the next morning (06:00 h to 07:00 h) as soon as the participants woke up.

2.5. Personal air pollution exposure

Data (May 2019–November 2021) regarding hourly ambient air pollution ($PM_{2.5}$ and NO_2) and daily weather conditions (temperature and relative humidity) were collected from 16 air monitoring stations of the Taiwan Environmental Protection Administration (<https://data.epa.gov.tw/>). The levels of personal exposure to ambient temperature and relative humidity were estimated using the data obtained from the air monitoring stations nearest to the participants. For each pollutant, the daily mean concentration values obtained from the 16 stations were averaged. Subsequently, the moving averages of the concentrations of air pollutants were calculated to adjust for temporal variations; the data lag was as follows: 1 day, 3 days, 5 days, 7 days, 1 month, 1 year, and 2 years. The spatial variations in the levels of personal exposure to air pollution were estimated using a validated land-use regression model (Li et al., 2021). Then, the annual mean of the residential exposure of each participant in 2019 was divided by the mean annual concentration of $PM_{2.5}$ or NO_2 in the same year to determine participants' spatial variations. In the aforementioned calculation (corresponding estimate of personal exposure evaluated through land use regression in 2019/annual mean air pollution level in 2019), land use variables, including population density and the vegetation index, were assumed to be associated with air pollution levels and to exhibit no substantial changes during the study period (Qiu et al., 2022). Finally, the levels of personal exposure were calculated by multiplying spatial variations (corresponding to each participant for an air pollutant) with moving averages. Therefore, the final calculation formula [(corresponding estimate of personal exposure evaluated through land use regression in 2019/annual mean air pollution level in 2019) \times the moving average level of each pollutant for lag days 0–1, 0–3, 0–5, 0–7, 0–30, 0–365, and 0–730] facilitated the spatiotemporal estimation of air pollution exposure levels, which helped to predict the air pollutant exposure from the personal exposure levels.

2.6. Statistical analysis

AHI exhibited a positively skewed distribution, so it is described in terms of median values (25th and 75th percentiles). Sleep parameters excluding AHI, environmental variables, and nocturnal changes in body composition showed a near-normal distribution. The nocturnal change (Δ) in each body composition parameter was calculated by subtracting the corresponding presleep value from the postsleep value. Differences between patients with different OSA severities in terms of demographical characteristics, polysomnography parameters, environmental factors, and nocturnal changes in body composition parameters were determined using a chi-square test for categorical variables, a two-sample *t*-test for continuous variables with a normal distribution, and the Mann–Whitney *U* test for continuous variables with a skewed distribution.

A generalized linear regression model was used to estimate the absolute values of nocturnal changes in body composition due to an interquartile range (IQR) increase in personal exposure to pollution. Age, sex, BMI, and neck and waist circumferences were included in the model as covariates. During the 3-year-long study period, the sleep parameters and exposure levels exhibited seasonality and long-term trends (Epstein et al., 2009; Mehra and Redline, 2008). Therefore, a natural spline with 3 degrees of freedom (*dfs*) per year at the date of participants' visit to the sleep center was included in the model to adjust for the effects of seasonality and long-term trends (Epstein et al., 2009). In addition, a natural spline with 3 *dfs* for exposure to mean temperature and relative humidity was included in the model to adjust for the potential nonlinear effects of weather conditions (Prediletto et al., 2021). The cumulative effects of air pollution (lag: 0–1 day, 0–3 days, 0–5 days, 0–7 days, 0–1 month, 0–1 year, and 0–2 years) were used to evaluate the short-, medium-, and long-term effects of air pollution on nocturnal changes in body compositions. A subgroup analysis was performed using an AHI value of 15 as the threshold (He et al., 2022). Using a two-pollutant model, a sensitivity analysis was performed to measure the robustness of the effects of air pollution on nocturnal changes in body composition (Qiu et al., 2022); $PM_{2.5}$ and NO_2 were incorporated in one model to estimate the absolute change in body compositions associated with an IQR increment with NO_2 (have controlled for $PM_{2.5}$) or $PM_{2.5}$ (have controlled for NO_2). A generalized logistic regression model was used to estimate the odds ratios (OR) to compare between patients with mild-OSA ($5 \leq AHI < 15$) and individuals without OSA ($AHI < 5$) (He et al., 2022).

Through partial least squares (PLS) regression, nocturnal changes in various body composition parameters were investigated to predict AHI in participants with AHI values < 15 . Here, PLS was not built between body compositions and AHI in mild-OSA patients with AHI between 5 and 15. This is because the OR to compare between patients with mild-OSA ($5 \leq AHI < 15$) and individuals without OSA ($AHI < 5$) need to be calculated associated with an IQR increment of comprehensive index predicted from the body composition parameters, and mild-OSA and non-OSA patients constituted this subgroup with $AHI < 15$.

In the present study, PLS regression was used because of its ability to address high levels of correlation between predictors. In PLS models including AHI as a continuous dependent variable, logarithmic transformation were performed after adding 1 to ensure normal distribution. PLS regression is superior in terms of dimension reduction; thus, the covariance between predictors and outcome variables is maximized (Boulesteix, 2004; Prunicki et al., 2020). The first step in PLS regression involved the incorporation of data regarding air pollution-induced nocturnal changes in body composition into the PLS model by using a cross-validation method to determine the optimal number of dimensions (latent variables). Five dimensions with the lowest cross-validation errors were identified, which were used (instead of the original individual predictors) in a leave-one-out cross-validation method to predict the best outcomes with a balanced underfitting–overfitting risk (Boulesteix, 2004). We also calculated the variable importance in projection (VIP) score for each predictor; a higher VIP score indicated higher relevance of a predictor in outcome prediction. For each participant, a comprehensive prediction value was calculated using

the body composition parameters. Multiple linear and logistic regression models adjusted for age and sex were fitted separately to investigate the effects of the prediction value on continuous AHI and the OR to compare between patients with mild-OSA and individuals without OSA. A two-sided *p* value of <0.05 indicated statistical significance. All analyses were performed using the “MASS” and “PLS” packages of R (version 3.5.3).

3. Results

This study included 3550 individuals (mean age, 47.6 ± 14.1 years; BMI, 26.7 ± 5.0 kg/m²). The median AHI value was 23.2 (IQR, 10.7–44.4). In participants with AHI values >15, various sleep indicators exhibited a worsening trend (Table 1). As shown in Fig. 1, the average levels of NO₂ and PM_{2.5} were considerably higher than the guidelines set by the World Health Organization (WHO; Ambient Air Quality Standards for NO₂ and PM_{2.5} were 10 µg/m³ and 5 µg/m³, respectively) in 2021 (Burki, 2021). Table 2 summarizes the nocturnal changes in the body composition of all participants, those with AHI values <15, and those with AHI values ≥ 15. The *p* values of the two-sample *t*-test used to compare the two subgroups with different AHI values indicated that nocturnal changes in lower-limb body compositions varied substantially between the two subgroups.

Nocturnal changes in the compositions of the whole body, trunk, and upper limbs were found not to be affected by NO₂ (Table S1) and PM_{2.5} (Table S2) in the one-pollutant model. However, nocturnal changes in lower-limb body composition were strongly associated with both short- and long-term exposures to NO₂ and PM_{2.5} (Table 3) in the one-pollutant model. After adjusting for age, sex, BMI, and waist and neck circumferences NO₂ and PM_{2.5}, respectively, affected nine and six lower-limb body composition parameters (Table 3). Specifically, increases in right leg fat percentage (RLFATP) and left leg fat mass (LLFATM) were associated with only short-term exposure to NO₂. Both short- and medium-term exposures to NO₂ increased left leg fat percentage (LLFATP). Whereas, short-, medium-, and long-term exposure to NO₂ could decreased the following four good parameters of body compositions, namely fat free mass of right leg (RLFFM), predicted muscle mass of right leg (RLPMM), fat free mass of left leg (LLFFM), and predicted muscle mass of left leg (LLPMM), but increased levels of the two bad indicators of body compositions impedance of right leg and left leg (RLIMP, LLIMP). By contrast,

PM_{2.5} exerted no effects on RLFFM and RLPMM. Nonetheless, short-term exposure to PM_{2.5} increased right leg fat mass (RLFATM). The number of parameters associated with only short-term PM_{2.5} exposure (RLFATP, RLFATM, LLFATP, and LLFATM) was higher than that associated with only short-term NO₂ exposure (RLFATP and LLFATM). Both short- and long-term exposures to PM_{2.5} decreased LLFFM and LLPMM. Notably, only two parameters, RLIMP and LLIMP, were strongly associated with short-, medium-, and long-term exposures to PM_{2.5}, whereas short-, medium-, and long-term exposures to NO₂ affected six parameters (RLFFM, RLPMM, RLIMP, LLFFM, LLPMM, and LLIMP). The effects of NO₂ on nocturnal changes in lower-limb body compositions were prominent in participants with AHI values <15 (Table 4) in the one-pollutant model; this remained unchanged after coexposure adjustment in the two-pollutant model (Table 5). By contrast, PM_{2.5} exerted almost no effects on the body composition of the participants in this subgroup, whether in the one-pollutant model or the two-pollutant model (Table 4 and Table 5). In participants with AHI values ≥ 15, only PM_{2.5} exerted slight effects on body composition in the one-pollutant model (Table S3). The subgroup with AHI values <15 comprised patients with mild-OSA and those without OSA, therefore we investigated whether the significant (*p* < .05) association between NO₂ and body composition observed in participants with AHI values <15 remained significant in patients with mild-OSA.; the results revealed that the significant associations were maintained in patients with mild-OSA in the one-pollutant model (Table S4).

A nonsignificant association was observed between air pollutants and AHI in all participants. We previously found that NO₂ exposure only affects individuals with AHI values <15 (He et al., 2022). In the present study, both short- and long-term exposures to NO₂ were associated with an increased risk of mild-OSA in the two-pollutant model (Fig. 2). Furthermore, both PM_{2.5} and NO₂ were strongly associated with nocturnal changes in body composition. NO₂ was also associated with an increased risk of mild-OSA. Then, we elucidated whether nocturnal changes in body composition were associated with OSA in patients with AHI <15, who are sensitive to air pollution. Participants with AHI values ≥ 15 were found to be unaffected by air pollution; it is meaningless to investigate the relationship between body composition and AHI in this subgroup, whose body compositions could not be used to link air pollution and AHI together. Hence, we focused only on those with AHI values <15.

Table 1

Demographic characteristics, sleep-related parameters, and environmental exposures at lag0 for patients from the sleep center in Taipei.

	Subgroup of patients			P-value ^b
	All patients (N = 3550)	AHI < 15 (N = 1200)	AHI ≥ 15 (N = 2350)	
Personal characteristics				
Age [years (mean ± SD)]	47.6 ± 14.1	43.7 ± 14.6	49.6 ± 13.3	<0.001
Male [N (%)]	2351 (66.2)	582 (48.5)	1769 (75.3)	<0.001
BMI [kg/m ² (mean ± SD)]	26.7 ± 5.0	24.2 ± 4.1	28.0 ± 4.9	<0.001
Neck [cm (mean ± SD)]	37.7 ± 3.3	36.0 ± 2.9	38.6 ± 3.1	<0.001
Waist [cm (mean ± SD)]	91.4 ± 11.3	85.2 ± 9.4	94.6 ± 11.1	<0.001
Sleep-related parameters				
TST [hr (mean ± SD)]	4.5 ± 1.0	4.6 ± 1.1	4.5 ± 1.0	0.002
Sleep efficiency [% (mean ± SD)]	74.2 ± 16.8	75.2 ± 16.8	73.7 ± 16.7	0.009
AHI {events/h [median (25th, 75th percentiles)]} ^a	23.2 (10.7, 44.4)	7.4 (3.5, 10.9)	35.4 (23.4, 57.6)	<0.001
Mean SpO2 [% (mean ± SD)]	94.9 ± 2.3	96.2 ± 1.5	94.2 ± 2.4	<0.001
Environmental factors				
PM _{2.5} [µg/m ³ (mean ± SD)]	13.7 ± 6.9	13.8 ± 7.0	13.6 ± 6.9	0.506
NO ₂ [ppb (mean ± SD)]	16.9 ± 6.9	17.1 ± 6.9	16.7 ± 6.9	0.146
Temperature [°C (mean ± SD)]	24.2 ± 5.2	24.2 ± 5.2	24.2 ± 5.2	0.909
Mean RH [% (mean ± SD)]	71.4 ± 8.8	71.3 ± 8.9	71.5 ± 8.8	0.608

Abbreviations: BMI, body mass index; TST, total sleep time; AHI, apnea-hypopnea index; SpO2, peripheral oxygen saturation; PM_{2.5}, particulate matter with aerodynamic diameter ≤ 2.5 µm; NO₂, nitrogen oxides; RH, relative humidity.

^a These variables are skewed distributed, described as median (25th, 75th percentiles), and logarithm transformation is performed on them in the test. Other variables are approximately normally distributed and described as mean (standard deviation).

^b P-values are obtained from two-sample *t*-test for continuous variables with normal distribution, from Mann Whitney *U* test for continuous variables with skewed distribution, and from Chi-square test for categorical variables to compare two OSA subgroups.

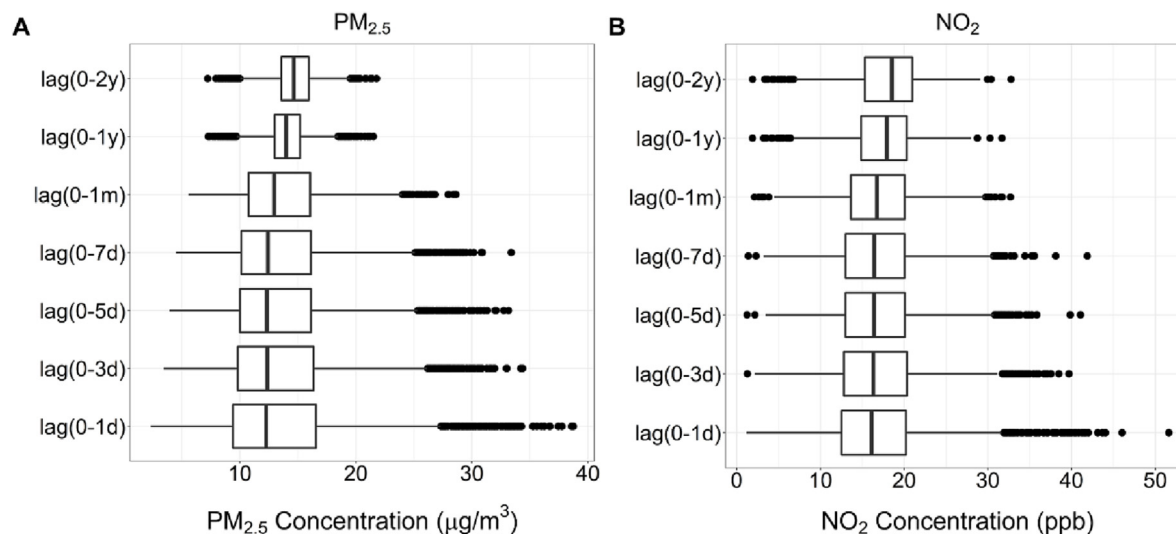


Fig. 1. The distribution of the personal exposure to both short-term and long-term ambient air pollution. Note: d, day; m, month; y, year.

In PLS regression, we used eight parameters (RLFATP, RLFFM, RLPMM, RLIMP, LLFATP, LLFFM, LLPMM, and LLIMP) exhibiting strong associations with NO_2 in different lags (Table 4). The VIP scores of LLIMP, LLPMM, LLFFM, and RLIMP exceeded 1, and the order was as follows: LLIMP > LLPMM > LLFFM > RLIMP (Fig. 3A). Higher VIP scores indicated better ability to predict outcomes. The coefficients of the aforementioned four parameters ranked in the top four in AHI prediction: LLIMP > RLIMP > LLFFM > LLPMM (Fig. 3B). Notably, these four parameters were associated with NO_2 in all lags of the two-pollutant model investigating NO_2 effects on overnight changes of body compositions in patients with AHI <15 (Table 5). This finding highlighted the importance of these four parameters and also the fact that NO_2 primarily affected these four body composition parameters, which, in turn, affected OSA. Using a PLS model including the eight body composition parameters as predictors and AHI as the outcome variable, we calculated a comprehensive prediction value for each participant. BMI and neck and waist circumferences were highly correlated with body composition, so we adjusted the model for age and sex. An IQR increase in the comprehensive prediction value estimated using the eight parameters markedly increased AHI by 17 % (95 % CI: 11.2–23.2) in participants with AHI values <15. In the logistic regression model, the OR for the comparison between patients with mild-OSA and individuals without OSA was 1.67 (95 % CI: 1.35–2.03).

4. Discussion

The findings of this study clarify the pathogenesis of air pollution-induced mild-OSA. By assessing nocturnal changes in the body composition of the participants, we found that air pollution increased the risk of mild-OSA; in addition, it increased nocturnal fat percentage and impedance but reduced nocturnal fat-free mass and muscle mass in the lower limbs of participants with AHI values <15. These effects persisted even after coexposure adjustment. Simultaneously, nocturnal changes in lower-limb body composition were significantly associated with increased risk of mild-OSA. Therefore, air pollution may have effects on mild-OSA by disrupting nocturnal body composition.

It has been reported by our previous study that air pollution, particularly NO_2 exposure, affects mild-OSA (He et al., 2022). In the present study, we validated our previous conclusion, although the moving averages of NO_2 level decreased from those in our previous study. The most common primary mechanisms through which air pollution affects OSA involve inflammation and oxidative stress. Air pollutants easily enter the respiratory tract and may disrupt the sinonasal epithelial barrier, resulting in nonallergic eosinophilic inflammation (Ramanathan et al., 2017). Irritation due to inflammation may decrease lung ventilation and perfusion, which

exacerbate the hypoxic events associated with OSA (Kleinman et al., 2008). However, our study is different from earlier studies because we found that NO_2 exposure aggravates mild-OSA, whereas other studies generally reported that patients with OSA or moderate-to-severe OSA are sensitive to air pollution (Billings et al., 2019; Cheng et al., 2019; Shen et al., 2018). Shen et al. (2018) reported that an IQR increase in the daily (6.8 ppb) and 1-year mean (2.7 ppb) NO_2 exposure levels is associated with 2.0 % and 3.6 % increases in the AHI value of all patients with OSA; $\text{PM}_{2.5}$ exposure also increased AHI. In the present study, both short- and long-term exposures to NO_2 were associated mild-OSA but not all OSA severities. By contrast, a multiethnic study conducted in the United States revealed that a 10-ppb annual increase and a 10-ppb 5-year increase in NO_2 exposure were strongly associated with 39 % and 41 % higher adjusted odds of OSA in patients with moderate to severe OSA (AHI ≥ 15) (Billings et al., 2019). Conversely, Cheng et al. (2019) found no association between NO_2 or $\text{PM}_{2.5}$ and OSA among all patients, including those with severe OSA (AHI ≥ 30); however, the concentrations of $\text{PM}_{2.5}$ (32.3 $\mu\text{g}/\text{m}^3$) and NO_2 (27.2 ppb) in their study were considerably higher than those in the present study. In our previous study, several explanations were provided for the association between air pollution and mild-OSA (He et al., 2022). In the present study, the mean BMI of participants with AHI values ≥ 15 was considerably higher than that of participants with AHI values <15 (Table 1). Fat deposits in tissues surrounding the upper airway tract increase its collapsibility, resulting in reduced chest compliance and functional residual capacity (Naiman and Cherniack, 1960; Shelton et al., 1993). Consequently, the oxygen demand increases, which predisposes individuals with obesity to apnea (Shelton et al., 1993). Furthermore, individuals with AHI values ≥ 15 not only have relatively high BMI but also are aged; they are vulnerable to various comorbidities, such as hypertension, congestive heart failure, atrial fibrillation, and diabetes (Senaratna et al., 2016), which can aggravate OSA; hence, a bidirectional relationship is evident between OSA and comorbidities. Thus, obesity and comorbidities highly contribute to the pathogenesis of moderate to severe OSA, thus masking the effects of air pollution on OSA.

In the present study, NO_2 and $\text{PM}_{2.5}$ were associated with nocturnal changes in the lower-limb body composition of all patients. The association between NO_2 and lower-limb body composition was maintained in participants with AHI values <15 but not in those with AHI values ≥ 15 ; by contrast, $\text{PM}_{2.5}$ affected neither of the two subgroups. The lower-limb body composition parameters affected by NO_2 were increased fat percentage, increased impedance, decreased fat-free mass and muscle mass. A Taiwanese study reported that an IQR increase in the average annual $\text{PM}_{2.5}$ concentration was associated with a 0.4-kg decrease in the muscle mass and 0.7-kg increase in the fat mass of the whole body; although $\text{PM}_{2.5}$ reduced fat-

Table 2

Overnight changes in body compositions for patients from sleep center in Taipei.

	Subgroup of patients			P-value ^a
	All patients (N = 3550)	AHI < 15 (N = 1200)	AHI ≥ 15 (N = 2350)	
The whole body				
Fat percentage, %	0.38 (1.85)	0.43 (1.76)	0.35 (1.89)	0.257
Fat mass, kg	0.04 (1.55)	0.09 (1.18)	0.01 (1.71)	0.081
Fat free mass, kg	−0.76 (1.37)	−0.71 (1.17)	−0.79 (1.46)	0.113
Predicted muscle mass, kg	−0.72 (1.29)	−0.67 (1.10)	−0.74 (1.38)	0.08
Visceral fat level, kg	0.08 (0.65)	0.06 (0.58)	0.09 (0.68)	0.121
Bone mass, kg	−0.04 (0.09)	−0.05 (0.08)	−0.04 (0.09)	0.317
Total body water, kg	−1.47 (1.56)	−1.13 (1.28)	−1.65 (1.66)	<0.001
Extracellular water, kg	−0.24 (0.39)	−0.19 (0.30)	−0.27 (0.43)	<0.001
Intracellular water, kg	−1.24 (1.21)	−0.95 (1.02)	−1.38 (1.28)	<0.001
Basal metabolic rate, kJ	−94.14 (158.43)	−85.18 (128.26)	−98.72 (171.65)	0.008
Metabolic age, year	0.62 (3.24)	0.53 (2.78)	0.66 (3.44)	0.236
Trunk				
Fat percentage, %	0.14 (2.28)	0.15 (2.20)	0.14 (2.32)	0.86
Fat mass, kg	0.34 (0.99)	0.25 (0.78)	0.39 (1.08)	<0.001
Fat free mass, kg	0.52 (1.21)	0.36 (1.06)	0.61 (1.27)	<0.001
Predicted muscle mass, kg	0.50 (1.14)	0.35 (0.99)	0.57 (1.20)	<0.001
Impedance, Ω	36.16 (23.91)	34.92 (25.63)	36.79 (22.97)	0.033
Phase angle, φ	0.11 (0.77)	0.08 (0.71)	0.12 (0.79)	0.106
Physique rating	−0.99 (4.65)	−0.94 (4.75)	−1.01 (4.61)	0.687
Upper limbs				
LAFATP, %	−0.55 (1.90)	−0.56 (2.01)	−0.55 (1.84)	0.882
LAFATM, kg	−0.05 (0.10)	−0.04 (0.08)	−0.06 (0.10)	<0.001
LAFFM, kg	−0.08 (0.14)	−0.05 (0.12)	−0.09 (0.14)	<0.001
LAPMM, kg	−0.07 (0.13)	−0.05 (0.11)	−0.09 (0.14)	<0.001
LAIMP, Ω	9.63 (18.68)	6.96 (20.39)	10.99 (17.59)	<0.001
RAFATP, %	−0.55 (1.71)	−0.59 (1.76)	−0.53 (1.69)	0.347
RAFATM, kg	−0.05 (0.09)	−0.03 (0.08)	−0.05 (0.09)	<0.001
RAFFM, kg	−0.06 (0.13)	−0.04 (0.11)	−0.08 (0.14)	<0.001
RAPMM, kg	−0.06 (0.13)	−0.04 (0.11)	−0.07 (0.14)	<0.001
RAIMP, Ω	6.87 (17.71)	4.44 (19.05)	8.11 (16.86)	<0.001
Lower limbs				
LLFATP, %	0.79 (1.53)	1.04 (1.50)	0.67 (1.53)	<0.001
LLFATM, kg	−0.11 (0.33)	−0.05 (0.25)	−0.14 (0.36)	<0.001
LLFFM, kg	−0.58 (0.31)	−0.51 (0.27)	−0.61 (0.32)	<0.001
LLPMM, kg	−0.54 (0.29)	−0.48 (0.26)	−0.58 (0.31)	<0.001
LLIMP, Ω	25.86 (12.49)	27.42 (13.17)	25.07 (12.05)	<0.001
RLFATP, %	0.78 (1.46)	1.02 (1.45)	0.65 (1.44)	<0.001
RLFATM, kg	−0.10 (0.32)	−0.03 (0.25)	−0.14 (0.35)	<0.001
RLFFM, kg	−0.56 (0.38)	−0.48 (0.43)	−0.61 (0.34)	<0.001
RLPMM, kg	−0.53 (0.36)	−0.45 (0.41)	−0.57 (0.33)	<0.001
RLIMP, Ω	24.80 (12.63)	26.26 (12.92)	24.05 (12.41)	<0.001

Abbreviations: FATP, fat percent; FATM, fat mass; FFM: fat free mass; PMM: predicted muscle mass; IMP: impedance; LL: left leg; RL: right leg.

^a P-values are obtained from two-sample *t*-test to compare two OSA subgroups.

free mass in the trunk and upper limbs but not in lower limbs, it increased body fat mass in all three parts (Chen et al., 2019). These findings are different from the present study in that both PM_{2.5} and NO₂ were found to be associated with body composition in all participants. Furthermore, this study assessed nocturnal changes in body composition, whereas in the aforementioned study, body composition was evaluated only once. Another study conducted in Taiwan focused on nocturnal changes in body composition and reported that the 1-year mean PM_{2.5} and NO₂ levels were associated with only a decrease in physique rating (Tung et al., 2021); however, it was found that a high number of body composition parameters were associated with pollutants in this study. Unlike Tung et al. (2021), who explored the effects of 1-year mean air pollution exposure on nocturnal changes in body compositions, we comprehensively investigated short-, medium-, and long-term effects of air pollution.

In the present study, impedance that reflects the resistance of electric current through the body was measured. The highest volume of body water is stored in muscles; thus, the body of a more muscular individual is expected to store more water, which corresponds to lower impedance (Kyle et al., 2004). To the best of our knowledge, this study is the first to reveal that NO₂ exposure is associated with an increase in lower-limb impedance; however, our knowledge regarding the underlying mechanisms

remains limited. Elevated impedance indicates decreased muscle mass, therefore the effects of NO₂ on impedance may be exerted through the same mechanism through which NO₂ affects other body composition parameters such as fat percentage, fat-free mass, and muscle mass. The most common mechanism involves the activation of local or systematic inflammation by proinflammatory cytokines induced by air pollutant inhalation, which may impair muscle protein synthesis and promote proteolysis (Lang et al., 2002; Schaap et al., 2006). Furthermore, excess nocturnal fat deposition augments the production of proinflammatory cytokines, which further exert adverse effects on muscle mass (Kalinkovich and Livshits, 2017). Notably, the association between air pollution and body composition remained significant (*p* < .05) only in those with AHI values <15, the individuals susceptible to mild-OSA under the effects of air pollution. Thus, air pollution may aggravate mild-OSA by changing nocturnal body composition. Furthermore, individuals with AHI values ≥ 15 are generally aged and have a high risk of chronic diseases, both of which are associated with skeletal muscle depletion and fat accumulation due to decreased production of anabolic hormones such as growth hormone, insulin-like growth hormone, and hormones essential for maintaining muscle mass (Wang and Bai, 2012). Therefore, in older individuals with AHI values ≥ 15, although air pollution may negatively affect muscle and fat, the effects can be

Table 3
The absolute overnight changes in body compositions of lower limbs (95 % CI) associated with an IQR increment of personal exposure in one-pollutant model for all the patients in different lags.

Lower limbs	NO ₂ exposure ^a	Lag(0-1d)						Lag(0-3d)						Lag(0-5d)						Lag(0-7d)						Lag(0-1 m)						Lag(0-1y)						Lag(0-2y)																																																																																																																																																																																																																																																																																																																																																																																																																																																																																																																																																																																													
		Lag(0-1d)		Lag(0-3d)		Lag(0-5d)		Lag(0-7d)		Lag(0-1 m)		Lag(0-1y)		Lag(0-2y)		Lag(0-1d)		Lag(0-3d)		Lag(0-5d)		Lag(0-7d)		Lag(0-1 m)		Lag(0-1y)		Lag(0-2y)		Lag(0-1d)		Lag(0-3d)		Lag(0-5d)		Lag(0-7d)		Lag(0-1 m)		Lag(0-1y)		Lag(0-2y)																																																																																																																																																																																																																																																																																																																																																																																																																																																																																																																																																																																									
ΔRLFATP, %	0.080 (0.019, 0.14) ^{**}	0.091 (0.024, 0.158) ^{**}		0.079 (0.012, 0.146) [*]		0.078 (0.01, 0.147) [*]		0.068 (−0.002, 0.138)		0.045 (−0.018, 0.107)		0.056 (−0.007, 0.12)		0.080 (0.019, 0.14) ^{**}		0.091 (0.024, 0.158) ^{**}		0.079 (0.012, 0.146) [*]		0.078 (0.01, 0.147) [*]		0.068 (−0.002, 0.138)		0.045 (−0.018, 0.107)		0.056 (−0.007, 0.12)		0.080 (0.019, 0.14) ^{**}		0.091 (0.024, 0.158) ^{**}		0.079 (0.012, 0.146) [*]		0.078 (0.01, 0.147) [*]		0.068 (−0.002, 0.138)		0.045 (−0.018, 0.107)		0.056 (−0.007, 0.12)																																																																																																																																																																																																																																																																																																																																																																																																																																																																																																																																																																																											
ΔRLFATM, kg	0.010 (−0.002, 0.022)	0.012 (−0.001, 0.025)		0.011 (−0.003, 0.024)		0.010 (−0.004, 0.023)		0.007 (−0.007, 0.021)		0.003 (−0.009, 0.016)		0.007 (−0.006, 0.019)		0.010 (−0.002, 0.022)		0.012 (−0.001, 0.025)		0.011 (−0.003, 0.024)		0.010 (−0.004, 0.023)		0.007 (−0.007, 0.021)		0.003 (−0.009, 0.016)		0.007 (−0.006, 0.019)		0.010 (−0.002, 0.022)		0.012 (−0.001, 0.025)		0.011 (−0.003, 0.024)		0.010 (−0.004, 0.023)		0.007 (−0.007, 0.021)		0.003 (−0.009, 0.016)		0.007 (−0.006, 0.019)																																																																																																																																																																																																																																																																																																																																																																																																																																																																																																																																																																																											
ΔRLFFM, kg	−0.020 (−0.036, −0.003) [*]	−0.018 (−0.036, 0.001)		−0.018 (−0.037, 0)		−0.019 (−0.037, 0)		−0.023 (−0.043, −0.004) [*]		−0.021 (−0.038, −0.003) [*]		−0.016 (−0.034, 0.001)		−0.019 (−0.037, 0)		−0.018 (−0.036, 0.001)		−0.018 (−0.037, 0)		−0.019 (−0.037, 0)		−0.023 (−0.043, −0.004) [*]		−0.021 (−0.038, −0.003) [*]		−0.016 (−0.034, 0.001)		−0.019 (−0.037, 0)		−0.018 (−0.036, 0.001)		−0.019 (−0.037, 0)		−0.023 (−0.043, −0.004) [*]		−0.021 (−0.038, −0.003) [*]		−0.016 (−0.034, 0.001)		−0.019 (−0.037, 0)		−0.023 (−0.043, −0.004) [*]																																																																																																																																																																																																																																																																																																																																																																																																																																																																																																																																																																																									
ΔRLPMM, kg	−0.019 (−0.035, −0.003) [*]	−0.017 (−0.035, 0.001)		−0.018 (−0.038, 0.003)		−0.018 (−0.038, 0.003)		−0.017 (−0.038, 0.004)		−0.017 (−0.038, 0.004)		−0.016 (−0.034, 0.001)		−0.019 (−0.037, 0)		−0.018 (−0.036, 0.001)		−0.018 (−0.037, 0)		−0.019 (−0.037, 0)		−0.022 (−0.041, −0.004) [*]		−0.021 (−0.038, −0.003) [*]		−0.016 (−0.034, 0.001)		−0.019 (−0.037, 0)		−0.018 (−0.036, 0.001)		−0.019 (−0.037, 0)		−0.022 (−0.041, −0.004) [*]		−0.021 (−0.038, −0.003) [*]		−0.016 (−0.034, 0.001)		−0.019 (−0.037, 0)		−0.022 (−0.041, −0.004) [*]																																																																																																																																																																																																																																																																																																																																																																																																																																																																																																																																																																																									
ΔRLIMP, Ω	0.854 (0.304, 1.405) ^{**}	0.842 (0.228, 1.455) ^{**}		0.858 (0.244, 1.471) ^{**}		0.873 (0.252, 1.494) ^{**}		0.880 (0.243, 1.518) ^{**}		0.866 (0.298, 1.434) ^{**}		0.785 (0.207, 1.363) ^{**}		0.854 (0.304, 1.405) ^{**}		0.842 (0.228, 1.455) ^{**}		0.858 (0.244, 1.471) ^{**}		0.873 (0.252, 1.494) ^{**}		0.880 (0.243, 1.518) ^{**}		0.866 (0.298, 1.434) ^{**}		0.785 (0.207, 1.363) ^{**}		0.854 (0.304, 1.405) ^{**}		0.842 (0.228, 1.455) ^{**}		0.858 (0.244, 1.471) ^{**}		0.873 (0.252, 1.494) ^{**}		0.880 (0.243, 1.518) ^{**}		0.866 (0.298, 1.434) ^{**}		0.785 (0.207, 1.363) ^{**}		0.854 (0.304, 1.405) ^{**}		0.842 (0.228, 1.455) ^{**}		0.858 (0.244, 1.471) ^{**}		0.873 (0.252, 1.494) ^{**}		0.880 (0.243, 1.518) ^{**}		0.866 (0.298, 1.434) ^{**}		0.785 (0.207, 1.363) ^{**}		0.854 (0.304, 1.405) ^{**}		0.842 (0.228, 1.455) ^{**}		0.858 (0.244, 1.471) ^{**}		0.873 (0.252, 1.494) ^{**}		0.880 (0.243, 1.518) ^{**}		0.866 (0.298, 1.434) ^{**}		0.785 (0.207, 1.363) ^{**}		0.854 (0.304, 1.405) ^{**}		0.842 (0.228, 1.455) ^{**}		0.858 (0.244, 1.471) ^{**}		0.873 (0.252, 1.494) ^{**}		0.880 (0.243, 1.518) ^{**}		0.866 (0.298, 1.434) ^{**}		0.785 (0.207, 1.363) ^{**}		0.854 (0.304, 1.405) ^{**}		0.842 (0.228, 1.455) ^{**}		0.858 (0.244, 1.471) ^{**}		0.873 (0.252, 1.494) ^{**}		0.880 (0.243, 1.518) ^{**}		0.866 (0.298, 1.434) ^{**}		0.785 (0.207, 1.363) ^{**}		0.854 (0.304, 1.405) ^{**}		0.842 (0.228, 1.455) ^{**}		0.858 (0.244, 1.471) ^{**}		0.873 (0.252, 1.494) ^{**}		0.880 (0.243, 1.518) ^{**}		0.866 (0.298, 1.434) ^{**}		0.785 (0.207, 1.363) ^{**}		0.854 (0.304, 1.405) ^{**}		0.842 (0.228, 1.455) ^{**}		0.858 (0.244, 1.471) ^{**}		0.873 (0.252, 1.494) ^{**}		0.880 (0.243, 1.518) ^{**}		0.866 (0.298, 1.434) ^{**}		0.785 (0.207, 1.363) ^{**}		0.854 (0.304, 1.405) ^{**}		0.842 (0.228, 1.455) ^{**}		0.858 (0.244, 1.471) ^{**}		0.873 (0.252, 1.494) ^{**}		0.880 (0.243, 1.518) ^{**}		0.866 (0.298, 1.434) ^{**}		0.785 (0.207, 1.363) ^{**}		0.854 (0.304, 1.405) ^{**}		0.842 (0.228, 1.455) ^{**}		0.858 (0.244, 1.471) ^{**}		0.873 (0.252, 1.494) ^{**}		0.880 (0.243, 1.518) ^{**}		0.866 (0.298, 1.434) ^{**}		0.785 (0.207, 1.363) ^{**}		0.854 (0.304, 1.405) ^{**}		0.842 (0.228, 1.455) ^{**}		0.858 (0.244, 1.471) ^{**}		0.873 (0.252, 1.494) ^{**}		0.880 (0.243, 1.518) ^{**}		0.866 (0.298, 1.434) ^{**}		0.785 (0.207, 1.363) ^{**}		0.854 (0.304, 1.405) ^{**}		0.842 (0.228, 1.455) ^{**}		0.858 (0.244, 1.471) ^{**}		0.873 (0.252, 1.494) ^{**}		0.880 (0.243, 1.518) ^{**}		0.866 (0.298, 1.434) ^{**}		0.785 (0.207, 1.363) ^{**}		0.854 (0.304, 1.405) ^{**}		0.842 (0.228, 1.455) ^{**}		0.858 (0.244, 1.471) ^{**}		0.873 (0.252, 1.494) ^{**}		0.880 (0.243, 1.518) ^{**}		0.866 (0.298, 1.434) ^{**}		0.785 (0.207, 1.363) ^{**}		0.854 (0.304, 1.405) ^{**}		0.842 (0.228, 1.455) ^{**}		0.858 (0.244, 1.471) ^{**}		0.873 (0.252, 1.494) ^{**}		0.880 (0.243, 1.518) ^{**}		0.866 (0.298, 1.434) ^{**}		0.785 (0.207, 1.363) ^{**}		0.854 (0.304, 1.405) ^{**}		0.842 (0.228, 1.455) ^{**}		0.858 (0.244, 1.471) ^{**}		0.873 (0.252, 1.494) ^{**}		0.880 (0.243, 1.518) ^{**}		0.866 (0.298, 1.434) ^{**}		0.785 (0.207, 1.363) ^{**}		0.854 (0.304, 1.405) ^{**}		0.842 (0.228, 1.455) ^{**}		0.858 (0.244, 1.471) ^{**}		0.873 (0.252, 1.494) ^{**}		0.880 (0.243, 1.518) ^{**}		0.866 (0.298, 1.434) ^{**}		0.785 (0.207, 1.363) ^{**}		0.854 (0.304, 1.405) ^{**}		0.842 (0.228, 1.455) ^{**}		0.858 (0.244, 1.471) ^{**}		0.873 (0.252, 1.494) ^{**}		0.880 (0.243, 1.518) ^{**}		0.866 (0.298, 1.434) ^{**}		0.785 (0.207, 1.363) ^{**}		0.854 (0.304, 1.405) ^{**}		0.842 (0.228, 1.455) ^{**}		0.858 (0.244, 1.471) ^{**}		0.873 (0.252, 1.494) ^{**}		0.880 (0.243, 1.518) ^{**}		0.866 (0.298, 1.434) ^{**}		0.785 (0.207, 1.363) ^{**}		0.854 (0.304, 1.405) ^{**}		0.842 (0.228, 1.455) ^{**}		0.858 (0.244, 1.471) ^{**}		0.873 (0.252, 1.494) ^{**}		0.880 (0.243, 1.518) ^{**}		0.866 (0.298, 1.434) ^{**}		0.785 (0.207, 1.363) ^{**}		0.854 (0.304, 1.405) ^{**}		0.842 (0.228, 1.455) ^{**}		0.858 (0.244, 1.471) ^{**}		0.873 (0.252, 1.494) ^{**}		0.880 (0.243, 1.518) ^{**}		0.866 (0.298, 1.434) ^{**}		0.785 (0.207, 1.363) ^{**}		0.854 (0.304, 1.405) ^{**}		0.842 (0.228, 1.455) ^{**}		0.858 (0.244, 1.471) ^{**}		0.873 (0.252, 1.494) ^{**}		0.880 (0.243, 1.518) ^{**}		0.866 (0.298, 1.434) ^{**}		0.785 (0.207, 1.363) ^{**}		0.854 (0.304, 1.405) ^{**}		0.842 (0.228, 1.455) ^{**}		0.858 (0.244, 1.471) ^{**}		0.873 (0.252, 1.494) ^{**}		0.880 (0.243, 1.518) ^{**}		0.866 (0.298, 1.434) ^{**}		0.785 (0.207, 1.363) ^{**}		0.854 (0.304, 1.405) ^{**}		0.842 (0.228, 1.455) ^{**}		0.858 (0.244, 1.471) ^{**}		0.873 (0.252, 1.494) ^{**}		0.880 (0.243, 1.518) ^{**}		0.866 (0.298, 1.434) ^{**}		0.785 (0.207, 1.363) ^{**}		0.854 (0.304, 1.405) ^{**}		0.842 (0.228, 1.455) ^{**}		0.858 (0.244, 1.471) ^{**}		0.873 (0.252, 1.494) ^{**}		0.880 (0.243, 1.518) ^{**}		0.866 (0.298, 1.434) ^{**}		0.785 (0.207, 1.363) ^{**}		0.854 (0.304, 1.405) ^{**}		0.842 (0.228, 1.455) ^{**}		0.858 (0.244, 1.471) ^{**}		0.873 (0.252, 1.494) ^{**}		0.880 (0.243, 1.518) ^{**}		0.866 (0.298, 1.434) ^{**}		0.785 (0.207, 1.363) ^{**}		0.854 (0.304, 1.405) ^{**}		0.842 (0.228, 1.455) ^{**}		0.858 (0.244, 1.471) ^{**}		0.873 (0.252, 1.494) ^{**}		0.880 (0.243, 1.518) ^{**}		0.866 (0.298, 1.434) ^{**}		0.785 (0.207, 1.363) ^{**}		0.854 (0.304, 1.405) ^{**}		0.842 (0.228, 1.455) ^{**}		0.858 (0.244, 1.471) ^{**}		0.873 (0.252, 1.494) ^{**}		0.880 (0.243, 1.518) ^{**}		0.866 (0.298, 1.434) ^{**}		0.785 (0.207, 1.363) ^{**}		0.854 (0.304, 1.405) ^{**}		0.842 (0.228, 1.455) ^{**}		0.858 (0.244, 1.471) ^{**}		0.873 (0.252, 1.494) ^{**}		0.880 (0.243, 1.518) ^{**}		0.866 (0.298, 1.434) ^{**}		0.785 (0.207, 1.363) ^{**}		0.854 (0.304, 1.405) ^{**}		0.842 (0.228, 1.455) ^{**}		0.858 (0.244, 1.471) ^{**}		0.873 (0.252, 1.494) ^{**}		0.880 (0.243, 1.518) ^{**}		0.866 (0.298, 1.434) ^{**}		0.785 (0.207, 1.363) ^{**}		0.854 (0.304, 1.405) ^{**}		0.842 (0.228, 1.455) ^{**}		0.858 (0.244, 1.471) ^{**}		0.873 (0.252, 1.494) ^{**}		0.880 (0.243, 1.518) ^{**}		0.866 (0.298, 1.434) ^{**}		0.785 (0.207, 1.363) ^{**}		0.854 (0.304, 1.405) ^{**}		0.842 (0.228, 1.455) ^{**}		0.858 (0.244, 1.471) ^{**}		0.873 (0.252, 1.494) ^{**}		0.880 (0.243, 1.518) ^{**}		0.866 (0.298, 1.434) ^{**}		0.785 (0.207, 1.363) ^{**}		0.854 (0.304, 1.405) ^{**}		0.842 (0.228, 1.455) ^{**}		0.858 (0.244, 1.471) ^{**}		0.873 (0.252, 1.494) ^{**}		0.880 (0.243, 1.518) ^{**}		0.866 (0.298, 1.434) ^{**}		0.785 (0.207, 1.363) ^{**}		0.854 (0.304, 1.405) ^{**}		0.842 (0.228, 1.455) ^{**}		0.858 (0.244, 1.471) ^{**}		0.873 (0.252, 1.494) ^{**}		0.880 (0.243, 1.518) ^{**}		0.866 (0.298, 1.434) ^{**}		0.785 (0.207, 1.363) ^{**}		0.854 (0.304, 1.405) ^{**}		0.842 (0.228, 1.455) ^{**}		0.858 (0.244, 1.471) ^{**}		0.873 (0.252, 1.494) ^{**}		0.880 (0.243, 1.518) ^{**}		0.866 (0.298, 1.434) ^{**}		0.785 (0.207, 1.363) ^{**}		0.854 (0.304, 1.405) ^{**}		0.842 (0.228, 1.455) ^{**}		0.858 (0.244, 1.471) ^{**}		0.873 (0.252, 1.494) ^{**}		0.880 (0.243, 1.518) ^{**}		0.866 (0.298, 1.434) ^{**}		0.785 (0.207, 1.363) ^{**}		0.854 (0.304, 1.405) ^{**}		0.842 (0.228, 1.455) ^{**}		0.858 (0.244, 1.471) ^{**}		0.873 (0.252, 1.494) ^{**}		0.880 (0.243, 1.518) ^{**}		0.866 (0.298, 1.434) ^{**}		0.785 (0.207, 1.363) ^{**}		0.854 (0.304, 1.405) ^{**}		0.842 (0.228, 1.455) ^{**}		0.858 (0.244, 1.471) ^{**}		0.873 (0.252, 1.494) ^{**}		0.880 (0.243, 1.518) ^{**}		0.866 (0.298, 1.434) ^{**}		0.785 (0.207, 1.363) ^{**}		0.854 (0.304, 1.405) ^{**}		0.842 (0.228, 1.455) ^{**}		0.858 (0.244, 1.471) ^{**}		0.873 (0.252, 1.494) ^{**}		0.880 (0.243, 1.518) ^{**}		0.866 (0.298, 1.434) ^{**}		0.785 (0.207, 1.363) ^{**}		0.854 (0.304, 1.405) ^{**}		0.842 (0.228, 1.455) ^{**}		0.858 (0.244, 1.471) ^{**}		0.873 (0.252, 1.494) ^{**}		0.880 (0.243, 1.518) ^{**}		0.866 (0.298, 1.434) ^{**}		0.785 (0.207, 1.363) ^{**}		0.854 (0.304, 1.405) ^{**}		0.842 (0.228, 1.455) ^{**}		0.858 (0.244, 1.471) ^{**}		0.873 (0.252, 1.494) ^{**}		0.880 (0.243, 1.518) ^{**}		0.866 (0.298, 1.434) ^{**}		0.785 (0.207, 1.363) ^{**}		0.854 (0.304, 1.405) ^{**}		0.842 (0.228, 1.455) ^{**}		0.858 (0.244, 1.471) ^{**}		0.873 (0.252, 1.494) ^{**}		0.880 (0.243, 1.518) ^{**}		0.866 (0.298, 1.434) ^{**}		0.785 (0.207, 1.363) ^{**}		0.854 (0.304, 1.405) ^{**}		0.842 (0.228, 1.455) ^{**}		0.858 (0.244, 1.471) ^{**}		0.873 (0.252, 1.494) ^{**}		0.880 (0.243, 1.518) ^{**}		0.866 (0.298, 1.434) ^{**}		0.785 (0.207, 1.363) ^{**}		0.854 (0.304, 1.405) ^{**}		0.842 (0.228, 1.455) ^{**}		0.858 (0.244, 1.471) ^{**}		0.873 (0.252, 1.494) ^{**}		0.880 (

Abbreviations: RLFATP, right leg fat percentage; RLFFM, right leg fat free mass; RLPMM, right leg predicted muscle mass; RLIMP, right leg fat free mass; LLPMM, left leg predicted muscle mass; LLIMP, left leg impedance. NO₂, nitrogen oxides. Generalized linear regression model was performed while adjusting for the long-term trend, seasonality, weather conditions, and essential characteristics of participants (age, sex, BMI, neck, and waist circumference).

^a 'd' for day, 'm' for month, and 'y' for year.

* Indicates the significance level < 0.05.

** Indicates the significance level < 0.01.

*** Indicates the significance level < 0.001.

Table 4
The absolute overnight changes in body compositions of lower limbs (95 % CI) associated with an IQR increment of personal exposure in one-pollutant model for patients with AHI <15 in different lags.

Lower limbs	NO ₂ exposure ^a							
		Lag(0-1d)	Lag(0-3d)	Lag(0-5d)	Lag(0-7d)	Lag(0-1 m)	Lag(0-1y)	Lag(0-2y)
ΔRLFATP, %	0.118 (0.015, 0.222)*	0.158 (0.045, 0.272)**	0.119 (0.007, 0.231)*	0.124 (0.009, 0.238)*	0.065 (−0.052, 0.181)	0.056 (−0.05, 0.162)	0.044 (−0.061, 0.149)	
ΔRLFATM, kg	0.007 (−0.009, 0.024)	0.012 (−0.006, 0.031)	0.005 (−0.013, 0.023)	0.005 (−0.014, 0.023)	−0.005 (−0.024, 0.014)	−0.004 (−0.021, 0.013)	−0.004 (−0.021, 0.013)	
ΔRLFFM, kg	−0.038 (−0.073, −0.002)*	−0.041 (−0.08, −0.002)*	−0.046 (−0.084, −0.007)*	−0.049 (−0.088, −0.009)*	−0.054 (−0.094, −0.013)**	−0.042 (−0.079, −0.005)*	−0.032 (−0.068, 0.004)	
ΔRLPMM, kg	−0.036 (−0.07, −0.003)*	−0.039 (−0.076, −0.002)*	−0.043 (−0.080, −0.007)*	−0.046 (−0.083, −0.008)*	−0.052 (−0.09, −0.013)**	−0.041 (−0.075, −0.006)*	−0.032 (−0.066, 0.003)	
ΔRLIMP, Ω	1.659 (0.684, 2.634)***	1.483 (0.412, 2.555)**	1.518 (0.463, 2.573)**	1.673 (0.594, 2.753)**	1.098 (−0.005, 2.201)	1.090 (0.094, 2.086)*	0.954 (−0.040, 1.949)	
ΔLRFATP, %	0.124 (0.016, 0.232)*	0.155 (0.036, 0.274)*	0.110 (−0.007, 0.228)	0.115 (−0.005, 0.235)	0.086 (−0.036, 0.208)	0.069 (−0.042, 0.179)	0.055 (−0.055, 0.166)	
ΔLRFATM, kg	0.012 (−0.005, 0.028)	0.017 (−0.001, 0.035)	0.011 (−0.007, 0.028)	0.011 (−0.007, 0.029)	0.004 (−0.015, 0.022)	0.001 (−0.016, 0.017)	0 (−0.017, 0.017)	
ΔLRLFFM, kg	−0.031 (−0.05, −0.012)**	−0.029 (−0.049, −0.008)**	−0.029 (−0.05, −0.009)**	−0.032 (−0.053, −0.012)**	−0.030 (−0.051, −0.008)**	−0.028 (−0.047, −0.009)**	−0.025 (−0.044, −0.006)*	
ΔLRLPMM, kg	−0.029 (−0.047, −0.011)**	−0.027 (−0.047, −0.008)**	−0.027 (−0.047, −0.008)**	−0.030 (−0.050, −0.01)**	−0.028 (−0.048, −0.007)**	−0.026 (−0.044, −0.007)**	−0.023 (−0.041, −0.005)*	
ΔLRLIMP, Ω	1.721 (0.732, 2.709)***	1.387 (0.301, 2.472)*	1.338 (0.270, 2.406)*	1.465 (0.371, 2.559)**	1.374 (0.258, 2.489)*	1.287 (0.274, 2.300)*	1.157 (0.1480, 2.166)*	
Lower limbs	PM _{2.5} exposure ^a							
	Lag(0-1d)	Lag(0-3d)	Lag(0-5d)	Lag(0-7d)	Lag(0-1 m)	Lag(0-1y)	Lag(0-2y)	
ΔRLFATP, %	0.093 (−0.016, 0.201)	0.148 (0.025, 0.270)*	0.118 (−0.013, 0.248)	0.131 (−0.007, 0.268)	−0.008 (−0.186, 0.171)	0.074 (−0.030, 0.179)	0.078 (−0.034, 0.189)	
ΔRLFATM, kg	0.013 (−0.005, 0.030)	0.017 (−0.002, 0.037)	0.011 (−0.010, 0.032)	0.011 (−0.011, 0.033)	−0.007 (−0.036, 0.022)	0.012 (−0.005, 0.028)	0.013 (−0.005, 0.031)	
ΔRLFFM, kg	−0.005 (−0.042, 0.032)	−0.025 (−0.067, 0.017)	−0.028 (−0.074, 0.017)	−0.036 (−0.084, 0.012)	−0.039 (−0.101, 0.023)	−0.018 (−0.054, 0.019)	−0.010 (−0.049, 0.028)	
ΔRLPMM, kg	−0.006 (−0.041, 0.029)	−0.024 (−0.064, 0.016)	−0.028 (−0.070, 0.015)	−0.034 (−0.079, 0.011)	−0.037 (−0.096, 0.022)	−0.016 (−0.05, 0.018)	−0.010 (−0.046, 0.027)	
ΔRLIMP, Ω	0.891 (−0.132, 1.914)	0.929 (−0.223, 2.081)	1.008 (−0.223, 2.239)	1.234 (−0.064, 2.533)	0.521 (−1.174, 2.216)	0.606 (−0.378, 1.589)	0.571 (−0.481, 1.623)	
ΔLRFATP, %	0.091 (−0.022, 0.205)	0.136 (0.009, 0.264)*	0.105 (−0.031, 0.242)	0.124 (−0.021, 0.268)	0.018 (−0.169, 0.205)	0.060 (−0.050, 0.169)	0.064 (−0.053, 0.180)	
ΔLRFATM, kg	0.009 (−0.009, 0.026)	0.016 (−0.004, 0.035)	0.010 (−0.011, 0.031)	0.012 (−0.010, 0.033)	−0.004 (−0.032, 0.024)	0.007 (−0.010, 0.024)	0.008 (−0.010, 0.026)	
ΔLRLFFM, kg	−0.019 (−0.039, 0.001)	−0.017 (−0.039, 0.005)	−0.017 (−0.04, 0.007)	−0.024 (−0.049, 0.001)	−0.020 (−0.052, 0.013)	−0.013 (−0.032, 0.006)	−0.011 (−0.031, 0.009)	
ΔLRLPMM, kg	−0.019 (−0.038, 0)	−0.016 (−0.037, 0.005)	−0.014 (−0.036, 0.009)	−0.020 (−0.044, 0.004)	−0.016 (−0.047, 0.015)	−0.009 (−0.027, 0.009)	−0.007 (−0.027, 0.012)	
ΔLRLIMP, Ω	0.985 (−0.052, 2.023)	0.788 (−0.378, 1.955)	0.845 (−0.400, 2.090)	1.119 (−0.196, 2.434)	0.967 (−0.749, 2.682)	0.441 (−0.560, 1.442)	0.424 (−0.644, 1.493)	

Abbreviations: RLFATP, right leg fat percentage; RLFFM, right leg fat free mass; RLPMM, right leg predicted muscle mass; RLIMP, right leg fat free mass; LLPMM, left leg predicted muscle mass; LLPMP, left leg impedance; LLPATP, left leg fat percent; LLPFM, left leg fat free mass; LLPMM, left leg predicted muscle mass; LLPMP, left leg impedance. NO₂, nitrogen oxides. Generalized linear regression model was performed while.

adjusting for the long-term trend, seasonality, weather conditions, and essential characteristics of participants (age, sex, BMI, neck, and waist circumference).

^a 'd' for day, 'm' for month, and 'y' for year.

* Indicates the significance level < 0.05.

** Indicates the significance level < 0.01.

*** Indicates the significance level < 0.001.

Table 5
The absolute overnight changes in body compositions of lower limbs (95 % CI) associated with an IQR increment of personal exposure in two-pollutant model for patients with AHI <15 in different lags.

Lower limbs	NO ₂ exposure ^a						
	Lag(0-1d)	Lag(0-3d)	Lag(0-5d)	Lag(0-7d)	Lag(0-1 m)	Lag(0-1y)	Lag(0-2y)
ΔRLFATP, %	0.104 (−0.018, 0.226)	0.124 (−0.008, 0.257)	0.088 (−0.039, 0.216)	0.098 (−0.031, 0.228)	0.101 (−0.032, 0.233)	0.023 (−0.101, 0.146)	0.009 (−0.113, 0.131)
ΔRLFATM, kg	0.001 (−0.020, 0.021)	0.006 (−0.016, 0.028)	−0.001 (−0.022, 0.020)	−0.001 (−0.022, 0.021)	−0.004 (−0.025, 0.018)	−0.014 (−0.035, 0.006)	−0.014 (−0.034, 0.006)
ΔRLFFM, kg	−0.048 (−0.090, −0.007)*	−0.039 (−0.085, 0.006)	−0.045 (−0.088, −0.001)*	−0.047 (−0.091, −0.003)*	−0.051 (−0.096, −0.006)*	−0.047 (−0.089, −0.004)*	−0.039 (−0.081, 0.003)
ΔRLPMM, kg	−0.045 (−0.085, −0.006)*	−0.037 (−0.080, 0.006)	−0.042 (−0.083, −0.001)*	−0.044 (−0.086, −0.002)*	−0.049 (−0.092, −0.007)*	−0.046 (−0.086, −0.006)*	−0.038 (−0.078, 0.001)
ΔRLIMP, Ω	1.731 (0.531, 2.930)**	1.510 (0.206, 2.813)*	1.531 (0.271, 2.791)*	1.666 (0.392, 2.939)*	1.580 (0.276, 2.884)*	1.506 (0.300, 2.713)*	1.362 (0.163, 2.561)*
ΔLLFATP, %	0.114 (−0.013, 0.242)	0.129 (−0.010, 0.268)	0.082 (−0.052, 0.216)	0.091 (−0.044, 0.227)	0.117 (−0.022, 0.255)	0.052 (−0.077, 0.181)	0.035 (−0.093, 0.163)
ΔLLFATM, kg	0.009 (−0.01, 0.029)	0.013 (−0.008, 0.035)	0.006 (−0.014, 0.027)	0.006 (−0.015, 0.027)	0.005 (−0.016, 0.026)	−0.004 (−0.024, 0.015)	−0.005 (−0.025, 0.015)
ΔLLFFM, kg	−0.029 (−0.052, −0.006)*	−0.027 (−0.051, −0.003)*	−0.027 (−0.051, −0.003)*	−0.029 (−0.053, −0.005)*	−0.034 (−0.059, −0.009)*	−0.033 (−0.056, −0.010)**	−0.031 (−0.053, −0.008)**
ΔLLPMM, kg	−0.026 (−0.048, −0.005)*	−0.026 (−0.05, −0.002)*	−0.027 (−0.050, −0.004)*	−0.029 (−0.052, −0.006)*	−0.034 (−0.057, −0.01)*	−0.032 (−0.054, −0.010)**	−0.030 (−0.052, −0.008)**
ΔLLIMP, Ω	1.744 (0.524, 2.964)**	1.470 (0.145, 2.795)*	1.374 (0.091, 2.657)*	1.488 (0.191, 2.785)**	1.805 (0.480, 3.130)*	1.951 (0.723, 3.180)**	1.796 (0.578, 3.014)**
PM _{2.5} exposure ^a							
ΔRLFATP, %	0.029 (−0.099, 0.156)	0.082 (−0.051, 0.215)	0.081 (−0.058, 0.220)	0.077 (−0.066, 0.220)	0.014 (−0.165, 0.192)	0.085 (−0.035, 0.205)	0.086 (−0.042, 0.215)
ΔRLFATM, kg	0.009 (−0.012, 0.03)	0.017 (−0.004, 0.039)	0.021 (−0.002, 0.044)	0.021 (−0.002, 0.045)	0.020 (−0.010, 0.049)	0.023 (0.003, 0.043)	0.024 (0.003, 0.046)
ΔRLFFM, kg	0.021 (−0.022, 0.064)	0.008 (−0.037, 0.054)	0.018 (−0.030, 0.065)	0.014 (−0.035, 0.063)	0.042 (−0.019, 0.103)	0.012 (−0.029, 0.053)	0.013 (−0.030, 0.057)
ΔRLPMM, kg	0.018 (−0.023, 0.059)	0.008 (−0.035, 0.051)	0.017 (−0.028, 0.061)	0.014 (−0.032, 0.060)	0.042 (−0.015, 0.100)	0.012 (−0.026, 0.051)	0.014 (−0.027, 0.055)
ΔRLIMP, Ω	0.088 (−1.164, 1.340)	0.437 (−0.875, 1.75)	0.007 (−1.363, 1.377)	0.148 (−1.264, 1.560)	−0.958 (−2.717, 0.801)	−0.207 (−1.392, 0.979)	−0.225 (−1.492, 1.043)
ΔLLFATP, %	0.019 (−0.114, 0.153)	0.073 (−0.066, 0.212)	0.072 (−0.074, 0.217)	0.068 (−0.083, 0.218)	0.011 (−0.176, 0.198)	0.058 (−0.068, 0.184)	0.057 (−0.078, 0.192)
ΔLLFATM, kg	0.001 (−0.020, 0.021)	0.009 (−0.013, 0.03)	0.012 (−0.01, 0.035)	0.013 (−0.010, 0.036)	0.009 (−0.020, 0.038)	0.013 (−0.006, 0.032)	0.013 (−0.008, 0.034)
ΔLLFFM, kg	−0.004 (−0.028, 0.020)	−0.006 (−0.031, 0.019)	0.006 (−0.02, 0.032)	0.002 (−0.025, 0.029)	0.021 (−0.012, 0.054)	0.006 (−0.017, 0.028)	0.006 (−0.018, 0.030)
ΔLLPMM, kg	−0.005 (−0.028, 0.017)	−0.004 (−0.028, 0.019)	0.009 (−0.016, 0.034)	0.006 (−0.020, 0.031)	0.024 (−0.008, 0.056)	0.009 (−0.012, 0.031)	0.010 (−0.013, 0.033)
ΔLLIMP, Ω	0.097 (−1.178, 1.371)	0.457 (−0.879, 1.793)	−0.049 (−1.444, 1.346)	0.077 (−1.361, 1.515)	−1.075 (−2.863, 0.713)	−0.568 (−1.772, 0.637)	−0.612 (−1.900, 0.676)

Abbreviations: RLFATP, right leg fat percentage; RLFFM, right leg fat free mass; RLPMM, right leg predicted muscle mass; RLIMP, right leg impedance; LLFATP, left leg fat percent; LLFFM, left leg fat free mass; LLPMM, left leg predicted muscle mass; LLIMP, left leg impedance. Generalized linear regression model was performed while adjusting for the long-term trend, seasonality, weather conditions, and essential characteristics of participants (age, sex, BMI, neck, and waist circumference).

^a 'd' for day, 'm' for month, and 'y' for year.

* Indicates the significance level < 0.05.

** Indicates the significance level < 0.01.

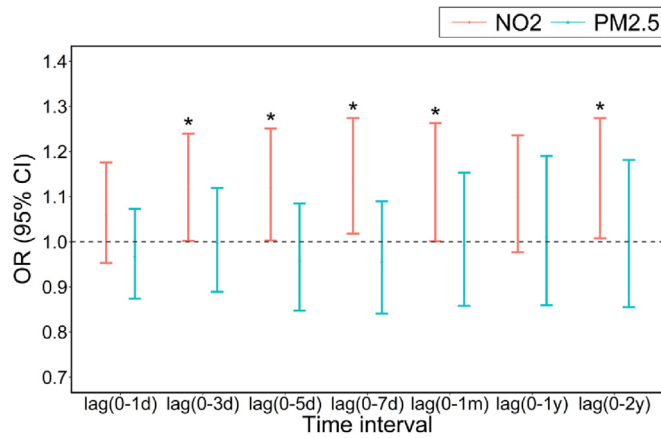


Fig. 2. Odds ratio (95%CI) of mild OSA associated with an IQR increment of personal pollution exposure, compared with non-OSA patients in two-pollutant models by lags. Generalized logistic model was performed while adjusting for the long-term trend, seasonality, weather conditions, and essential characteristics of participants (age, sex, BMI, neck and waist circumference). Note: IQR, interquartile range; PM_{2.5}, particulate matter with aerodynamic diameter $\leq 2.5 \mu\text{m}$; NO₂, nitrogen oxides; d, day; m, month; y, year; * indicates the significance level < 0.05 .

overshadowed by the effects of aging, chronic disease, and physical inactivity. In the present study, the effects of air pollution on body composition were prominent in younger individuals with relatively low AHI values.

In participants with AHI values < 15 , air pollution was associated with both AHI and nocturnal changes in lower-limb body composition. Taken together, it was then demonstrated that these body compositions associated with air pollution, were also associated with OSA by PLS model. PLS regression can easily address multicollinearity problems in situations where multiple explanatory variables are correlated with each other (Kemalbay and Korkmazoglu, 2012). Through PLS regression, a linear regression model was constructed including eight body composition parameters and log transformed AHI. The contribution of each component to AHI was indicated by the regression coefficients and VIP scores, both of which identified LLIMP, LLPMM, LLFFM, and RLIMP to be the top four important

parameters contributing to OSA pathogenesis. These four parameters were strongly associated with NO₂ in all lags (Table 5), which further corroborates their importance in OSA pathogenesis. Thus, air pollution aggravates OSA by primarily affecting the aforementioned four parameters; nonetheless, a causal relationship remains to be established. OSA severity is associated with decreased muscle mass (Kosacka et al., 2013; Matsumoto et al., 2018; Sauleda et al., 2003; Tung et al., 2021), increased body fat (Lovin et al., 2010; Stevens et al., 2020; Tung et al., 2021), and nocturnal rostral fluid shift (Yumino et al., 2010). Two potential mechanisms were elucidated underlying the association between body composition and OSA. The first can be attributed to a sedentary lifestyle combined with increased venous pressure, which results in fluid accumulation in the legs during the day and a large rostral shift in the volume of this fluid (from the legs to the neck and lungs) at night (Peppard and Young, 2004). Thus, nocturnal rostral fluid shift may be a cause of OSA. Nonetheless, OSA may be a cause, rather than an effect, of rostral fluid shift because under obstructive conditions, negative pressure inside the thorax may cause fluid movement from the legs. In the present study, increased lower-limb impedance after air pollution exposure indicates nocturnal decreases in muscle mass and water volume in the legs, which in turn is associated with AHI. Moreover, the coefficient and VIP score of impedance were found to be the highest, which suggests that this is the predominant mechanism mediating the association between body composition and OSA. Unfortunately, establishing a causal relationship between nocturnal changes in body composition and OSA was difficult because of data limitations. Another mechanism claims that sleep structure disorders and reduced slow-wave sleep may impair the secretion of pulsatile growth hormone, which regulates muscle synthesis (Karimi et al., 2010). This finding is supported by findings of this study regarding the nocturnal accumulation of fat and loss of muscle in the lower limbs of patients with sleep disorders. Exposure to air pollution aggravates this condition. Furthermore, long-term OSA has been associated with severe health problems, such as sarcopenia (Chen et al., 2019). The mechanism underlying air pollution-induced OSA appears to be intricate; air pollution may be directly associated with OSA or deteriorate OSA by disrupting nocturnal body composition.

The present study has some strengths. First, unlike earlier studies in which body composition was measured only once, it was measured twice (presleep and postsleep); nocturnal changes were assessed to dynamically reflect the association between OSA and body composition.

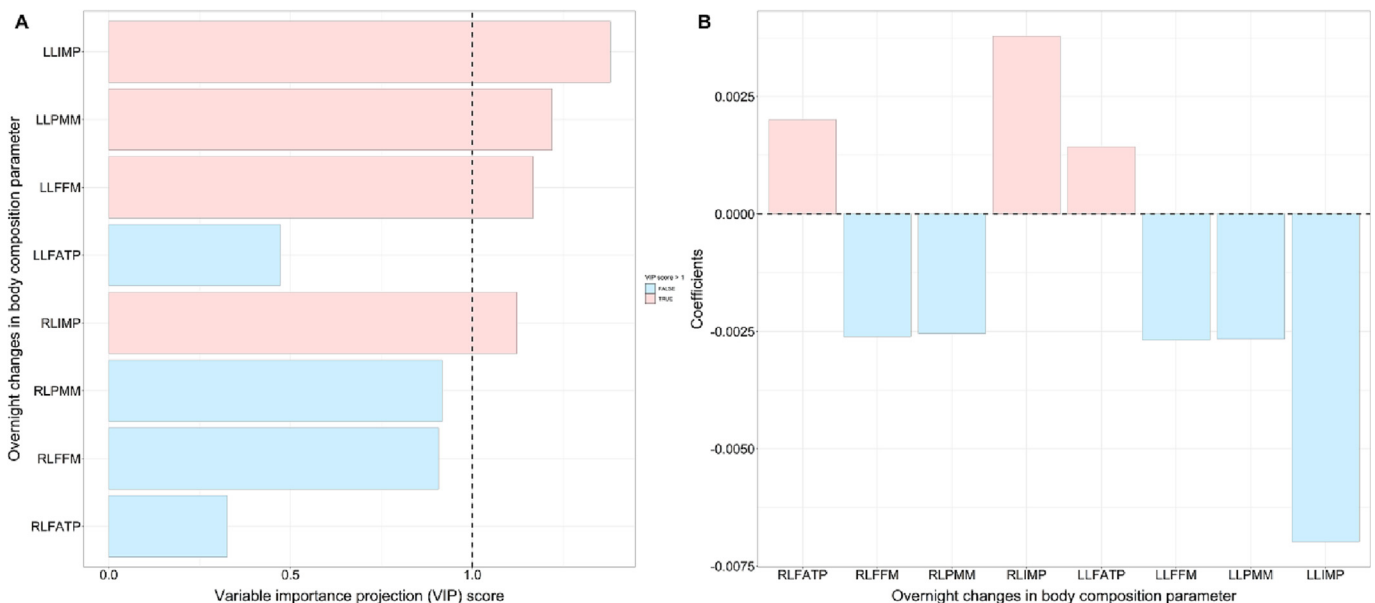


Fig. 3. Variable importance projection score and the coefficients of overnight changes in each body composition parameter in partial least square regression model with logarithm transformed AHI as dependent variable. Note: RLFATP, right leg fat percentage; RLFFM, right leg fat free mass; RLPMM, right leg predicted muscle mass; RLIMP, right leg impedance; LLFATP, left leg fat percent; LLFFM, left leg fat free mass; LLPMM, left leg predicted muscle mass; LLIMP, left leg impedance.

Furthermore, instead of focusing on the association between individual indicators and OSA, PLS regression was performed to address the collinearity between multiple body composition parameters and evaluate their combined effects on OSA. Third, the effects of short-, medium-, and long-term exposures to air pollution on OSA and body composition were investigated. Finally, using a land-use regression model, we estimated each participant's personal exposure to air pollution.

Our study has some limitations. This was a cross-sectional study conducted in an Asian population. Hence, it was difficult to identify any causal relationships between air pollution and body composition or between body composition and OSA. Furthermore, the findings may not be generalizable beyond the study population. In the future, cohort studies should be conducted to clarify the mediating role of body composition in the pathophysiology of OSA.

5. Conclusions

PM_{2.5} was found to be only associated with nocturnal changes in lower-limb body composition but not with mild-OSA. Both short- and long-term exposures to NO₂ were associated with mild OSA. Nocturnal changes in RLIMP, LLIMP, LLFFM, and LLPMM were not only significantly associated with all exposure windows of NO₂, but also ranked top four in predicting OSA; the parameter with the highest contribution to the association of body composition and OSA was the nocturnal increase in impedance. Therefore, NO₂ exposure exacerbates mild OSA by disrupting nocturnal changes such as inducing nocturnal fat accumulation and muscle depletion in the lower-limb body composition of patients with AHI values <15.

CRediT authorship contribution statement

Yansu He: Data curation, Formal analysis, Writing – original draft preparation, Writing – review & editing. **Wen-Te Liu:** Writing – review & editing. **Shang-Yang Lin:** The integrity and accuracy of the data. **Zhiyuan Li:** The application of the land-use regression and the accuracy of the exposure assessment. **Hong Qiu:** The integrity and accuracy of the data. **Steve Huang-Lam Yim:** The application of the land-use regression and the accuracy of the exposure assessment. **Hsiao-Chi Chuang:** Writing – review & editing, Methodology. **Kin Fai Ho:** Conceptualization, Methodology, Supervision, Writing - review & editing, Project administration, Funding acquisition.

Data availability

Data will be made available on request.

Declaration of competing interest

The authors declare that they have no known competing financial interests or personal relationships that could have appeared to influence the work reported in this paper.

Acknowledgements

The authors acknowledge all the participants and administrators in this study.

Funding

This study was supported by the Vice-Chancellors Discretionary Fund of The Chinese University of Hong Kong (project no.: 4930744).

Appendix A. Supplementary data

Supplementary data to this article can be found online at <https://doi.org/10.1016/j.scitotenv.2023.163969>.

References

- Billings, M.E., Gold, D., Szpiro, A., Aaron, C.P., Jorgensen, N., Gassett, A., et al., 2019. The association of ambient air pollution with sleep apnea: the multi-ethnic study of atherosclerosis. *Ann. Am. Thorac. Soc.* 16, 363–370. <https://doi.org/10.1513/AnnalsATS.201804-248OC>.
- Boulesteix, A.L., 2004. PLS dimension reduction for classification with microarray data. *Stat. Appl. Genet. Mol. Biol.* 3, Article33. <https://doi.org/10.2202/1544-6115.1075>.
- Burki, T., 2021. WHO introduces ambitious new air quality guidelines. *Lancet* 398, 1117. [https://doi.org/10.1016/S0140-6736\(21\)002126-7](https://doi.org/10.1016/S0140-6736(21)002126-7).
- Chen, C.H., Huang, L.Y., Lee, K.Y., Wu, C.D., Chiang, H.C., Chen, B.Y., et al., 2019. Effects of PM_{2.5} on skeletal muscle mass and body fat mass of the elderly in Taipei, Taiwan. *Sci. Rep.* 9, 11176. <https://doi.org/10.1038/s41598-019-47576-9>.
- Cheng, W.J., Liang, S.J., Huang, C.S., Lin, C.L., Pien, L.C., Hang, L.W., 2019. Air pollutants are associated with obstructive sleep apnea severity in non-rapid eye movement sleep. *J. Clin. Sleep Med.* 15, 831–837. <https://doi.org/10.5664/jcsm.7830>.
- Chuang, K.J., Chan, C.C., Su, T.C., Lee, C.T., Tang, C.S., 2007. The effect of urban air pollution on inflammation, oxidative stress, coagulation, and autonomic dysfunction in young adults. *Am. J. Respir. Crit. Care Med.* 176, 370–376. <https://doi.org/10.1164/rccm.200611-1627OC>.
- Epstein, L.J., Kristo, D., Strollo Jr., P.J., Friedman, N., Malhotra, A., Patil, S.P., et al., 2009. Clinical guideline for the evaluation, management and long-term care of obstructive sleep apnea in adults. *J. Clin. Sleep Med.* 5, 263–276. <https://doi.org/10.5664/jcsm.27497>.
- He, Y., Liu, W., Lin, S., Li, Z., Qiu, H., Yim, S.H.L., et al., 2022. Association of traffic air pollution with severity of obstructive sleep apnea in urban areas of Northern Taiwan: a cross-sectional study. *Sci. Total Environ.* 827. <https://doi.org/10.1016/j.scitotenv.2022.154347>.
- Jordan, A.S., McSharry, D.G., Malhotra, A., 2014. Adult obstructive sleep apnoea. *Lancet* 383, 736–747. [https://doi.org/10.1016/S0140-6736\(13\)60734-5](https://doi.org/10.1016/S0140-6736(13)60734-5).
- Kalinkovich, A., Livshits, G., 2017. Sarcopenic obesity or obese sarcopenia: a cross talk between age-associated adipose tissue and skeletal muscle inflammation as a main mechanism of the pathogenesis. *Ageing Res. Rev.* 35, 200–221. <https://doi.org/10.1016/j.arr.2016.09.008>.
- Karimi, M., Koranyi, J., Franco, C., Peker, Y., Eder, D.N., Angelhed, J.E., et al., 2010. Increased neck soft tissue mass and worsening of obstructive sleep apnea after growth hormone treatment in men with abdominal obesity. *J. Clin. Sleep Med.* 6, 256–263. <https://doi.org/10.5664/jcsm.27823>.
- Kasai, T., Bradley, T.D., Friedman, O., Logan, A.G., 2014. Effect of intensified diuretic therapy on overnight rostral fluid shift and obstructive sleep apnoea in patients with uncontrolled hypertension. *J. Hypertens.* 32, 673–680. <https://doi.org/10.1097/HJH.0000000000000047>.
- Kemalbay, G., Korkmazoglu, O.B., 2012. Effects of multicollinearity on electricity consumption forecasting using partial least squares regression. *Procedia Soc. Behav. Sci.* 62, 1150–1154. <https://doi.org/10.1016/j.sbspro.2012.09.197>.
- Kleinman, M.T., Araujo, J.A., Nel, A., Sioutas, C., Campbell, A., Cong, P.Q., et al., 2008. Inhaled ultrafine particulate matter affects CNS inflammatory processes and may act via MAP kinase signaling pathways. *Toxicol. Lett.* 178, 127–130. <https://doi.org/10.1016/j.toxlet.2008.03.001>.
- Kosacka, M., Korzeniewska, A., Jankowska, R., 2013. The evaluation of body composition, adiponectin, C-reactive protein and cholesterol levels in patients with obstructive sleep apnea syndrome. *Adv. Clin. Exp. Med.* 22, 817–824.
- Kyle, U.G., Bosaeus, I., De Lorenzo, A.D., Deurenberg, P., Elia, M., Gómez, J.M., et al., 2004. Bioelectrical impedance analysis—part I: review of principles and methods. *Clin. Nutr.* 23, 1226–1243. <https://doi.org/10.1016/j.clnu.2004.06.004>.
- Lang, C.H., Frost, R.A., Naim, A.C., MacLean, D.A., Vary, T.C., 2002. TNF- α impairs heart and skeletal muscle protein synthesis by altering translation initiation. *Am. J. Physiol. Endocrinol. Metab.* 282, E336–E347. <https://doi.org/10.1152/ajpendo.00366.2001>.
- Lemos, T., Gallagher, D., 2017. Current body composition measurement techniques. *Curr. Opin. Endocrinol. Diabetes Obes.* 24, 310–314. <https://doi.org/10.1097/med.0000000000000360>.
- Li, Z., Ho, K.F., Chuang, H.C., Yim, S.H.L., 2021. Development and intercity transferability of land-use regression models for predicting ambient PM₁₀, PM_{2.5}, NO₂ and O₃ concentrations in northern Taiwan. *Atmos. Chem. Phys.* 21, 5063–5078. <https://doi.org/10.5194/acp-21-5063-2021>.
- Lovin, S., Bercea, R., Cojocaru, C., Rusu, G., Mihăescu, T., 2010. Body composition in obstructive sleep apnoeahypopnea syndrome bio-impedance reflects the severity of sleep apnea. *Multidiscip. Respir. Med.* 5, 44–49. <https://doi.org/10.1186/2049-6958-5-1-44>.
- Matsumoto, T., Tanizawa, K., Tachikawa, R., Murase, K., Minami, T., Inouchi, M., et al., 2018. Associations of obstructive sleep apnea with truncal skeletal muscle mass and density. *Sci. Rep.* 8, 6550. <https://doi.org/10.1038/s41598-018-24750-z>.
- Mehra, R., Redline, S., 2008. Sleep apnea: a proinflammatory disorder that coaggregates with obesity. *J. Allergy Clin. Immunol.* 121, 1096–1102. <https://doi.org/10.1016/j.jaci.2008.04.002>.
- Naimark, A., Cherniack, R.M., 1960. Compliance of the respiratory system and its components in health and obesity. *J. Appl. Physiol.* 15, 377–382. <https://doi.org/10.1152/jappl.1960.15.3.377>.
- Park, J.G., Ramar, K., Olson, E.J., 2011. Updates on definition, consequences, and management of obstructive sleep apnea. *Mayo Clin. Proc.* 86, 549–554 quiz 554–545. <https://doi.org/10.4065/mcp.2010.0810 quiz 554-545>.
- Peppard, P.E., Young, T., 2004. Exercise and sleep-disordered breathing: an association independent of body habitus. *Sleep* 27, 480–484. <https://doi.org/10.1093/sleep/27.3.480>.
- Prediletto, I., Tavalazzi, F., Perziano, M., Fanfulla, F., Fabiani, A., Oldani, S., et al., 2021. Sleep features in Lymphangioliomyomatosis and their relationship with disease severity: a pilot study. *Sleep Med.* 85, 60–65. <https://doi.org/10.1016/j.sleep.2021.06.038>.
- Prunicki, M., Cauwenberghs, N., Ataam, J.A., Movassagh, H., Kim, J.B., Kuznetsova, T., et al., 2020. Immune biomarkers link air pollution exposure to blood pressure in adolescents. *Environ. Health* 19, 108. <https://doi.org/10.1186/s12940-020-00662-2>.
- Punjabi, N.M., 2008. The epidemiology of adult obstructive sleep apnea. *Proc. Am. Thorac. Soc.* 5, 136–143. <https://doi.org/10.1513/pats.200709-155MG>.
- Qiu, H., Liu, W.T., Lin, S.Y., Li, Z.Y., He, Y.S., Yim, S.H.L., et al., 2022. Association of air pollution exposure with low arousal threshold obstructive sleep apnea: a cross-sectional

- study in Taipei, Taiwan. *Environ. Pollut.* 306, 119393. <https://doi.org/10.1016/j.envpol.2022.119393>.
- Ramanathan Jr., M., London Jr., N.R., Tharakan, A., Surya, N., Sussan, T.E., Rao, X., et al., 2017. Airborne particulate matter induces nonallergic eosinophilic sinonasal inflammation in mice. *Am. J. Respir. Cell Mol. Biol.* 57, 59–65. <https://doi.org/10.1165/rcmb.2016-0351OC>.
- Redolfi, S., Yumino, D., Ruttanaumpawan, P., Yau, B., Su, M.C., Lam, J., et al., 2009. Relationship between overnight rostral fluid shift and obstructive sleep apnea in nonobese men. *Am. J. Respir. Crit. Care Med.* 179, 241–246. <https://doi.org/10.1164/rccm.200807-1076OC>.
- Reutrakul, S., Mokhlesi, B., 2017. Obstructive sleep apnea and diabetes: a state of the art review. *Chest* 152, 1070–1086.
- Ruehland, W.R., Rochford, P.D., O'Donoghue, F.J., Pierce, R.J., Singh, P., Thornton, A.T., 2009. The new AASM criteria for scoring hypopneas: impact on the apnea hypopnea index. *Sleep* 32, 150–157. <https://doi.org/10.1093/sleep/32.2.150>.
- Sauleda, J., García-Palmer, F.J., Tarraga, S., Maimó, A., Palou, A., Agustí, A.G., 2003. Skeletal muscle changes in patients with obstructive sleep apnoea syndrome. *Respir. Med.* 97, 804–810. [https://doi.org/10.1016/s0954-6111\(03\)00034-9](https://doi.org/10.1016/s0954-6111(03)00034-9).
- Schaap, L.A., Pluijm, S.M., Deeg, D.J., Visser, M., 2006. Inflammatory markers and loss of muscle mass (sarcopenia) and strength. *Am. J. Med.* 119. <https://doi.org/10.1016/j.amjmed.2005.10.049> 526.e529–517.
- Senaratna, C.V., English, D.R., Currier, D., Perret, J.L., Lowe, A., Lodge, C., et al., 2016. Sleep apnoea in Australian men: disease burden, co-morbidities, and correlates from the Australian longitudinal study on male health. *BMC Public Health* 16, 1029. <https://doi.org/10.1186/s12889-016-3703-8>.
- Shelton, K.E., Woodson, H., Gay, S., Suratt, P.M., 1993. Pharyngeal fat in obstructive sleep apnea. *Am. Rev. Respir. Dis.* 148, 462–466. <https://doi.org/10.1164/ajrccm/148.2.462>.
- Shen, Y.L., Liu, W.T., Lee, K.Y., Chuang, H.C., Chen, H.W., Chuang, K.J., 2018. Association of PM (2.5) with sleep-disordered breathing from a population-based study in Northern Taiwan urban areas. *Environ. Pollut.* 233, 109–113. <https://doi.org/10.1016/j.envpol.2017.10.052>.
- Stevens, D., Appleton, S., Vincent, A.D., Melaku, Y., Martin, S., Gill, T., et al., 2020. Associations of OSA and nocturnal hypoxemia with strength and body composition in community dwelling middle aged and older men. *Nat. Sci. Sleep* 12, 959–968. <https://doi.org/10.2147/NSS.S276932>.
- Su, S.Y., Liaw, Y.P., Jhuang, J.R., Hsu, S.Y., Chiang, C.J., Yang, Y.W., et al., 2019. Associations between ambient air pollution and cancer incidence in Taiwan: an ecological study of geographical variations. *BMC Public Health* 19, 1496. <https://doi.org/10.1186/s12889-019-7849-z>.
- Tung, N.T., Lee, Y.L., Lin, S.Y., Wu, C.D., Dung, H.B., Thuy, T.P.C., et al., 2021. Associations of ambient air pollution with overnight changes in body composition and sleep-related parameters. *Sci. Total Environ.* 791, 148265. <https://doi.org/10.1016/j.scitotenv.2021.148265>.
- Urbanik, D., Martynowicz, H., Mazur, G., Poreba, R., Gac, P., 2020. Environmental factors as modulators of the relationship between obstructive sleep apnea and lesions in the circulatory system. *J. Clin. Med.* 9. <https://doi.org/10.3390/jcm9030836>.
- Volpato, S., Bianchi, L., Cherubini, A., Landi, F., Maggio, M., Savino, E., et al., 2014. Prevalence and clinical correlates of sarcopenia in community-dwelling older people: application of the EWGSOP definition and diagnostic algorithm. *J. Gerontol. A Biol. Sci. Med. Sci.* 69, 438–446. <https://doi.org/10.1093/gerona/glt149>.
- Wang, C., Bai, L., 2012. Sarcopenia in the elderly: basic and clinical issues. *Geriatr Gerontol Int* 12, 388–396. <https://doi.org/10.1111/j.1447-0594.2012.00851.x>.
- Ward, L.C., 2019. Bioelectrical impedance analysis for body composition assessment: reflections on accuracy, clinical utility, and standardisation. *Eur. J. Clin. Nutr.* 73, 194–199. <https://doi.org/10.1038/s41430-018-0335-3>.
- Wong, A.L., Charpignon, M., Kim, H., Josef, C., de Hond, A.A.H., Foja, J.J., et al., 2021. Analysis of discrepancies between pulse oximetry and arterial oxygen saturation measurements by race and ethnicity and association with organ dysfunction and mortality. *JAMA Netw. Open* 4, e2131674. <https://doi.org/10.1001/jamanetworkopen.2021.31674>.
- Yumino, D., Redolfi, S., Ruttanaumpawan, P., Su, M.C., Smith, S., Newton, G.E., et al., 2010. Nocturnal rostral fluid shift: a unifying concept for the pathogenesis of obstructive and central sleep apnea in men with heart failure. *Circulation* 121, 1598–1605. <https://doi.org/10.1161/CIRCULATIONAHA.109.902452>.